Journal of Power Sources 195 (2010) 5508–5513

Contents lists available at ScienceDirect

Journal of Power Sources

journal homepage: www.elsevier.com/locate/jpowsour

Fabrication and evaluation of Ag-impregnated $BaCe_{0.8}Sm_{0.2}O_{2.9}$ composite cathodes for proton conducting solid oxide fuel cells

Tianzhi Wu, Yuanyuan Rao, Ranran Peng*, Changrong Xia

CAS Key Laboratory of Materials for Energy Conversion, Department of Material Science and Engineering, University of Science and Technology of China, JinZhai Road 96, Hefei, Anhui 230026, China

ARTICLE INFO

Article history:
Received 19 March 2010
Accepted 19 March 2010
Available online 25 March 2010

Keywords:
Silver
Cathode
Impregnation technique
Impedance spectroscopy

ABSTRACT

Ag–$BaCe_{0.8}Sm_{0.2}O_{2.9}$ (BCS) composite cathodes are fabricated by an ion impregnation technique in this work, and the effect of fabrication details on their electro-performance is studied. The firing temperature of impregnated Ag has little effect on Ag loading but has a great impact on the polarization resistances. When fired at 400 °C, the minimum polarization resistance for symmetric cells reaches 0.11 Ω cm^2 measured at 600 °C with an Ag loading of 0.40 mg cm^{-2}. When fired at 600 °C, the minimum polarization resistance is 29.73 Ω cm^2 at 600 °C with 0.24 mg cm^{-2} Ag-impregnated cathodes due to severe aggregation. The performance of Ag-impregnated cathodes is also compared with that of a $Sm_{0.5}Sr_{0.5}CoO_{3-\delta}$ (SSC) impregnated cathode. With the same volume ratio of 57%, the polarization resistance of an Ag-impregnated cathode is only about half of that for a SSC-impregnated cathode. Resistance simulation suggests that the reduction of low frequency resistances is the main reason for the decrease in polarization resistances in Ag-impregnated cathodes, which is consistent with its high oxygen diffusion coefficient. With a 57 vol.% Ag-impregnated cathode fired at 400 °C, the maximum power density of single cells is 283 mW cm^{-2} at 600 °C, about 16% larger than that for a 57 vol.% SSC-impregnated cathode.

1. Introduction

Protons conducting solid oxide fuel cells (H-SOFCs) have attracted much attention because of their unique characteristics, such as great efficiency in fuel utilization and suitability for operation at intermediate temperatures [1–3]. With proton conductors as electrolytes, water is formed at the cathodes. This makes the cathode reaction mechanisms particular from those with oxygen ion electrolytes and might lead to some special demands on the cathode materials.

Oxygen ion–electron mixed conductors are the most popular cathode materials for SOFCs with oxygen ion conducting electrolyte, and therefore, they are also investigated as cathode materials in H-SOFCs. Great power output has been achieved with oxygen ion–electron mixed conductors, such as $Ba_{0.5}Sr_{0.5}Co_{0.8}Fe_{0.2}O_3$ [3], $BaPr_{0.8}Gd_{0.2}O_{2.9}$ [4], $La_{0.6}Sr_{0.4}CoO_3$ [5], $Sm_xSr_{1-x}CoO_3$ [6], $Ba_{0.5}Sr_{0.5}Zn_{0.2}Fe_{0.8}O_{3-\delta}$ [7], $PrBaCo_2O_{5+\delta}$ [8] and $BaCe_{0.5}Bi_{0.5}O_3$ [9]. With $Ba_{0.5}Sr_{0.5}Zn_{0.2}Fe_{0.8}O_{3-\delta}$–$BaCe_{0.5}Zr_{0.3}Y_{0.16}Zn_{0.04}O_{3-\delta}$ as cathodes, the polarization resistance was 0.17 Ω cm^2 at 700 °C [7]. With $Sm_{0.5}Sr_{0.5}CoO_3$ (SSC)–$BaCe_{0.8}Sm_{0.2}O_{2.9}$ (BCS) as the composite cathode, the electrode polarization resistance was 0.21 Ω cm^2 at 700 °C and the maximum power output reached 240 mW cm^{-2} [6]. Intensive studies on SSC–BCS composite cathodes suggest that the migration of protons to TPBs and the surface diffusion of O_{ad}^- might be the two limiting reactions for H-SOFCs [10]. Therefore, exploring novel cathode materials with higher oxygen diffusion coefficients will be very helpful in reducing the polarization resistances, especially at intermediate temperatures.

Silver is a good electronic conductor and is a well-investigated catalyst for oxygen adsorption, dissociation and diffusion. The oxygen diffusion coefficient of Ag is 3.16×10^{-2} cm^2 s^{-1} at 427 °C [11], which is far better than that of SSC, only 8.6×10^{-7} cm^2 s^{-1} at 915 °C [12]. The high oxygen diffusion coefficient of Ag suggests that it might be a good cathode material for H-SOFCs [13]. However, the low melting point of Ag (962 °C) generally yields to a poor adhesion of the Ag-oxide composite electrodes to the electrolytes because it restricts the sintering temperature. In this work, an ion impregnation technique was adapted to fabricate an Ag–BCS composite cathode with BCS as the backbone and Ag coated on its inner surface. The electrochemical performance and the rate-limiting steps of such composite cathodes were investigated by impedance spectra analysis. Long-term stability was also studied with Ag-impregnated cathodes.

* Corresponding author. Tel.: +86 551 3600594; fax: +86 551 3607475.
E-mail address: pengrr@ustc.edu.cn (R. Peng).

0378-7753/$ – see front matter © 2010 Elsevier B.V. All rights reserved.
doi:10.1016/j.jpowsour.2010.03.063

2. Experimental

2.1. Fabrication of symmetric and single cells

$BaCe_{0.8}Sm_{0.2}O_{2.9}$ (BCS) powders were prepared by a glycine-nitrate process [3] and then cold-pressed into disc-type electrolyte substrates, followed by sintering at 1500 °C for 4 h in air. Porous BCS layers were deposited onto each surface of the electrolyte substrate by screen printing, and then sintered at 1300 °C for 4 h to form symmetric electrode backbones. The BCS backbones were about 100 μm in thickness and 11 mm in diameter. The impregnation solution of Ag^+ was prepared by dissolving $AgNO_3$ (99.9%, Aldrich) and glycine in distilled water with the glycine/Ag^+ molar ratio of 1:2. Ion impregnation was carried out by placing drops of the solution onto the surface of porous BCS backbones; the solution infiltrated into the pores of the backbone by capillary action [14–16]. After drying, the symmetric samples were fired at 400–600 °C in air for 2 h. The weight of Ag loaded on the BCS backbone was determined by an electronic balance (METTLER TOLEDO), and this impregnation step was repeated two to nine times to form symmetric cells with Ag–BCS composite electrodes.

Additionally, 90% Ag–5% Co_2O_3 co-impregnated cathodes were fabricated for comparison. $Co(NO_3)_2{\cdot}6H_2O$ and $AgNO_3$ were mixed and dissolved in distilled water with a stoichiometric ratio of 1:9, and then glycine was added, maintaining a glycine/metal molar ratio of 1:2. Ion impregnation was used to synthesize an Ag–Co_2O_3 co-impregnated cathode with the complex solution. The Ag–Co_2O_3 co-impregnated cathodes were fabricated by repeating the impregnation process seven times and consequent firing at 400, 500 and 600 °C for 2 h.

Single cells were prepared with anode supported configuration. NiO and BCS powders were mixed at a weight ratio of 65:35 as composite anode powders. Bilayers of NiO–BCS substrates and BCS electrolytes were fabricated by a co-pressing method, and they were then co-sintered at 1400 °C for 5 h. Ag–BCS composite cathodes were fabricated by the ion impregnation techniques described above. The thickness of the anode, electrolyte, and cathode layers were about 500, 70 and 100 μm, respectively.

2.2. Characterization

Ag paste was painted on the top of the cathodes as current collectors and was fired at 600 °C for 30 min. The electrochemical impedance spectra of the symmetric cells were obtained at temperatures from 600 to 300 °C in air at an electrochemical workstation (IM6e, Zahner). The AC impedance method was also used to investigate the electrochemical performance of single cells under open circuit conditions. The tested frequency range was from 0.01 Hz to 1 MHz with an amplitude of 10 mV. A scanning electron microscope (SEM, JSM-6700F, JEOL) was employed to investigate the morphology and distribution of the impregnated Ag particles. Single cells were tested from 400 to 600 °C in a home-developed testing system with humidified hydrogen (~3% H_2O) as the fuel and stationary air as the oxidant, respectively. The flow rate of humidified hydrogen was 50 ml min^{-1}. The discharging characters of single cells were also investigated using an IM6e electrochemical workstation.

3. Results and discussion

Fig. 1 shows the dependence of Ag loading on impregnation-firing cycles and their firing temperature. Ag loading did not appear to be affected by the firing temperature during the first seven cycles, which increased almost linearly with the cycle times and reached 0.44 ± 0.01 mg cm^{-2} after seven cycles. The increasing rate

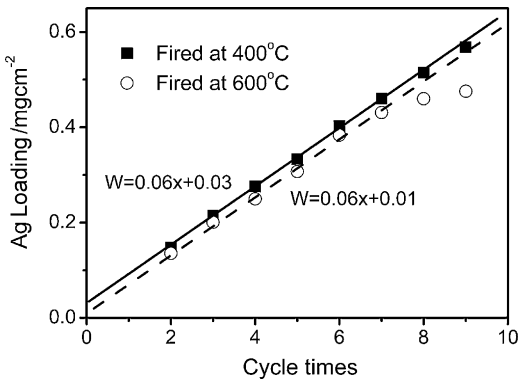

Fig. 1. Dependence of Ag loading on cycle times and firing temperature.

of the Ag loading was about 0.06 mg cm^{-2} for each cycle. With cycle times above seven, the Ag loading continued to increase for impregnated cathodes with Ag fired at 400 °C, while the value remained almost constant for those with Ag fired at 600 °C. The final Ag loadings for cathodes with Ag fired at 400 and 600 °C were 0.57 and 0.48 mg cm^{-2} after nine cycles, respectively.

Fig. 2 shows the dependence of polarization resistances on Ag loading and firing temperature. The polarization resistances were about 4691.16 Ω cm^2 at 400 °C for 0.14 mg cm^{-2} Ag-impregnated cathodes fired both at 400 and 600 °C. An increase in Ag loading led to a decrease in the polarization resistances of cathodes fired at both temperatures first, followed by a decrease. However, the Ag loading corresponding to minimum polarization is quite different for cathodes fired at different temperatures. For cathodes fired at 400 °C, the minimum polarization resistance is reached with the 0.40 mg cm^{-2} Ag-impregnated BCS cathodes, about 112.52 Ω cm^2 at 400 °C and 0.11 Ω cm^2 at 600 °C, respectively, which are 2–3 orders of magnitude lower than that with the 0.14 mg cm^{-2} Ag-impregnated cathodes. While minimum polarization resistances for cathodes fired at 600 °C are achieved with 0.24 mg cm^{-2} Ag-impregnated BSC cathodes, about 1521.49 Ω cm^2 at 400 °C and 29.73 Ω cm^2 at 600 °C, respectively. It should also be noted that the difference in polarization resistances of cathodes fired at different temperatures increased with Ag loading, as shown in Fig. 2. Ag loadings of 0.46 mg cm^{-2} (57 vol.%) yielded polarization resistances of 11,028.81 Ω cm^2 at 400 °C for impregnated cathodes fired

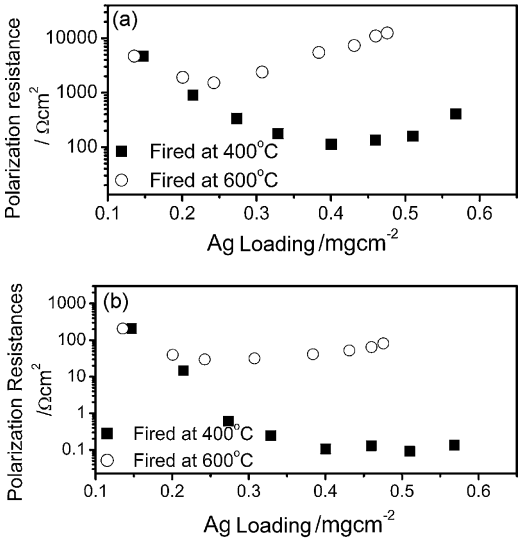

Fig. 2. Effect of the weight and firing temperature of impregnated Ag on polarization resistances for symmetric cells measured at (a) 400 °C and (b) 600 °C in air.

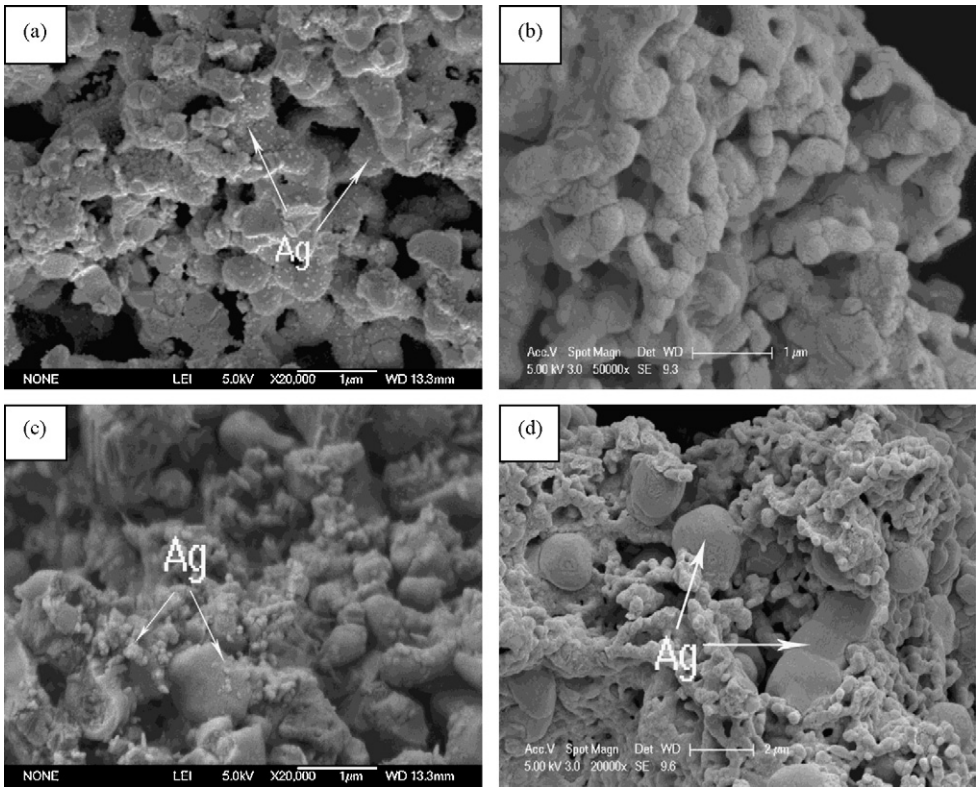

Fig. 3. SEM pictures of the impregnated electrodes with (a) 0.21 mg cm^{-2} Ag fired at 400 °C, (b) 0.46 mg cm^{-2} Ag fired at 400 °C, (c) 0.21 mg cm^{-2} Ag fired at 600 °C, and (d) 0.46 mg cm^{-2} Ag fired at 600 °C.

at 600 °C, about two orders larger than that fired at 400 °C, which is 0.13 Ω cm^2 at 600 °C.

SEM pictures of the fracture structures of impregnated cathodes with different Ag loadings that were fired at different temperatures are shown in Fig. 3 to explore the great difference in their polarization resistance. When the Ag loading was 0.21 mg cm^{-2} and the firing temperature was 400 °C, the Ag particles appeared discretely on BSC backbones, and the particle sizes of Ag and BCS were about 20 nm and 0.2–0.5 μm, respectively. With an increase in Ag loading, the amount of Ag particles on the BCS backbone increased, which gradually formed a complete cover, as shown in Fig. 3(b) with the 0.46 mg cm^{-2} Ag-impregnated BCS cathodes. This continuous microstructure greatly increases the triple phase boundaries (TPBs) and thus decreases the polarization resistance. With the 0.21 mg cm^{-2} Ag-impregnated cathode fired at 600 °C, the size of Ag particles increased to about 50–100 nm and was also isolated with each other on the BCS backbone, as shown in Fig. 3(c). However, when the Ag loading increased to 0.46 mg cm^{-2}, the Ag particles fired at 600 °C did not form a continuous cover but instead formed an aggregate, as shown in Fig. 3(d). This aggregation results in less TPBs and thus worse polarization resistances.

To better explore the effects of Ag loading and firing temperatures on polarization resistances, the impedance spectra of impregnated cathode are shown in Figs. 4 and 5. As shown in Fig. 4(a) and (b), three depressed arcs, peaking at 10^5, 3×10^3 and 70 Hz are observed in the impedance spectra for impregnated cathodes fired at 400 °C and measured at 400 °C, implying three rate-limiting processes. These impedance spectra were analyzed using an equivalent circuit composed of three RQ elements in series, $(R_HQ_H)(R_MQ_M)(R_LQ_L)$, to obtain the resistance of different processes, where R represents the polarization resistance, Q represents the constant phase element, and the subscripts H, M and L correspond to the frequency arcs. The resolved R_H, R_M and R_L at 400 °C are 112.85, 243.37 and 620.34 Ω cm^2, respectively, for 0.21 mg cm^{-2} Ag-impregnated cathodes and 2.54, 28.32 and 66.70 Ω cm^2, respectively, for 0.46 mg cm^{-2} Ag-impregnated cathodes. With an increase in Ag loading, all three frequency resistances reduce one or two orders, especially the low frequency resistances. The decrease in polarization resistance is in good accordance with the improvement of triple phase boundaries, as shown in Fig. 3. We have discussed the rate-limiting process for cathode reactions in proton conducting solid oxide fuel cells with $Sm_{0.5}Sr_{0.5}CoO_{3-\delta}$ and $BaCe_{0.8}Sm_{0.2}O_{3-\delta}$ composite cathodes, and we found that the high, middle, and low frequency arcs might correspond to the diffusion of protons from electrolytes to TPBs, the reduction of O_{ad} to O_{ad}^-, and the diffusion of O_{ad}^- to TPBs, respectively [10]. As shown in Fig. 4, the diffusion of O_{ad}^- to TPBs (corresponding to the low frequency arc) is the main resistive contributor to the polarization resistance, especially with the low Ag-loading impregnated cathode. Measured at 600 °C, only two arcs are observed in the spectra of both impregnated cathodes, as shown in Fig. 4(c) and (d), where high and middle frequency arcs could not be separated. In this case, two RQ elements were used to resolve the spectra, and the high and low frequency resistances were 3.49 and 9.19 Ω cm^2 for 0.21 mg cm^{-2} Ag-impregnated cathodes and 0.06 and 0.07 Ω cm^2 for 0.46 mg cm^{-2} Ag-impregnated cathodes.

The impedance spectra of 0.21 and 0.46 mg cm^{-2} Ag-impregnated cathodes fired at 600 °C and tested at 400 °C are shown in Fig. 5(a) and (b), respectively. Three arcs are also observed in these spectra with peak frequencies of 10^5, 5×10^3, and 10 Hz. Unlike those fired at 400 °C, R_H, R_M and R_L increase with an increase in Ag load due to severe aggregation of Ag particles, and thus a decrease of TPBs length. R_L, which corresponds to the transfer of O_{ad}^- to TPBs, is also the main contributor of polarization resistance at 400 °C. With the testing temperature enhanced to 600 °C, R_L is still the dominating resistance for 0.21 mg cm^{-2} Ag-impregnated cathodes, while R_H, which corresponds to the transfer of protons, becomes the primary contributor of polarization resistances for

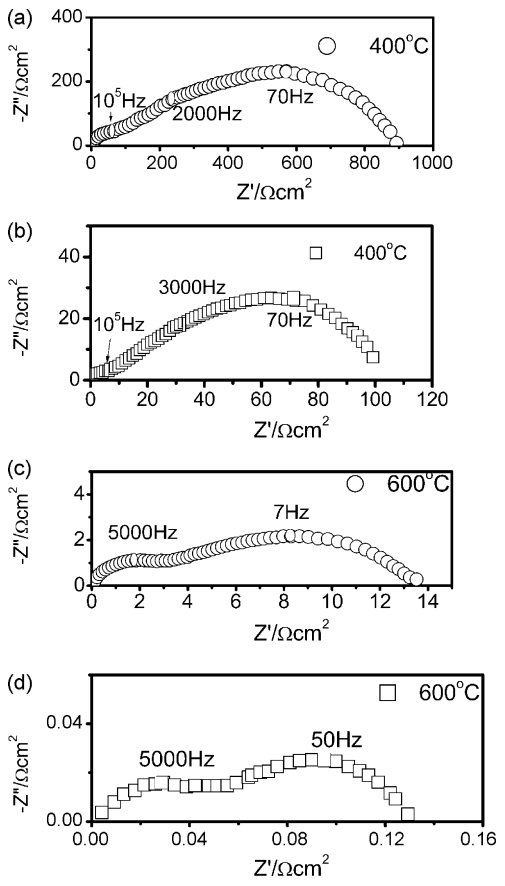

Fig. 4. Impedance spectra for symmetric cells with impregnated Ag fired at 400 °C and measured at 400 °C for Ag loadings of (a) 0.21 mg cm^{-2} and (b) 0.46 mg cm^{-2}, and measured at 600 °C for Ag loadings of (c) 0.21 mg cm^{-2} and (d) 0.46 mg cm^{-2}.

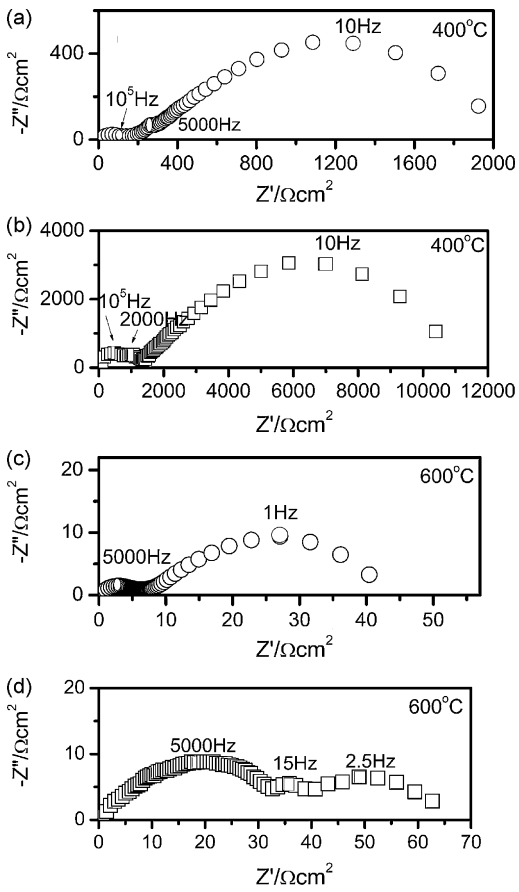

Fig. 5. Impedance spectra for symmetric cells with impregnated Ag fired at 600 °C and measured at 400 °C for Ag loadings of (a) 0.21 mg cm^{-2} and (b) 0.46 mg cm^{-2}, and measured at 600 °C for Ag loadings of (c) 0.21 mg cm^{-2} and (d) 0.46 mg cm^{-2}.

0.46 mg cm^{-2} Ag-impregnated cathodes, as shown in Fig. 5(c) and (d), respectively.

Fig. 6 shows the temperature dependence of simulated resistances with Ag-impregnated cathodes fired at 400 °C, in which R_M is fitted with the testing temperatures below 500 °C. All the three curves have good linear shape. The simulated activation energies for R_H increase with Ag loading by about 0.84 eV for 0.21 mg cm^{-2} and 0.91 eV for 0.46 mg cm^{-2} Ag-impregnated cathodes. Such activation energies for R_H are slightly higher than the activation energies of proton conduction, which is about 0.50–0.60 eV [17,18]. This might be caused by lattice distortion of external BCS due to the great surface absorbability of nano-sized Ag. The simulated activation energies for R_M and R_L, respectively, are 0.97 and 1.11 eV for 0.21 mg cm^{-2} Ag-impregnated cathodes, and 1.07 and 1.79 eV for 0.46 mg cm^{-2} Ag-impregnated cathodes.

The temperature dependence of simulated resistances with 0.46 mg cm^{-2} Ag-impregnated cathodes fired at 600 °C is shown in Fig. 7. The activation energies of such cathodes are calculated as 0.66, 0.89 and 1.32 eV for R_H, R_M and R_L, respectively. The activation energy for R_H is similar to the activation energy of proton conduction in doped $BaCeO_3$ [17,18], supporting our foregoing postulate that the high activation energy for R_H with Ag-impregnated cathodes fired at 400 °C might result from the great surface absorbability of nano-sized Ag.

The impedance spectra of symmetric cells with the 0.29 mg cm^{-2} SSC-impregnated cathode (SSC-IM) are shown in Fig. 8 as comparison [15]. The volume ratio of SSC in impregnated cathode is 57 vol.%, the same as that of Ag in a 0.46 mg cm^{-2} Ag-impregnated cathode. It can be seen that with the same volume ratio, the polarization resistance of an SSC-impregnated cathode is 0.24 Ω cm^2 at 600 °C, about twice that for Ag-impregnated cathode. The simulated high and low frequency resistances are 0.08 and 0.16 Ω cm^2 for SSC-impregnated cathodes and 0.06 and 0.07 Ω cm^2 for Ag-impregnated cathodes, suggesting that the reduction of low frequency resistances is the main reason for the decrease of polarization resistances in Ag-impregnated cathodes. This might result from the high oxygen transfer coefficient of Ag.

The electrochemical performance of Ag- and SSC-impregnated cathodes with the same ratio of 57 vol.% was also characterized

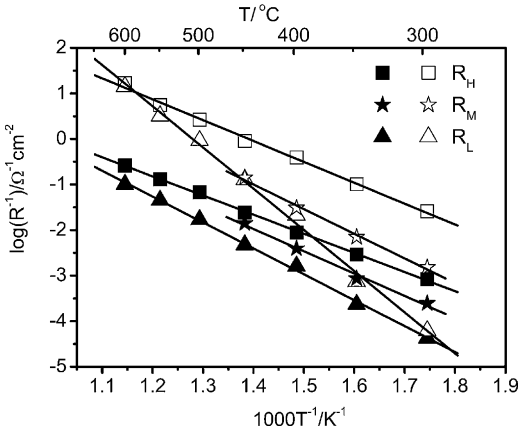

Fig. 6. Temperature dependence of fitted high frequency resistances (□, ■), middle frequency resistances (☆,★), and low frequency resistances (△, ▲) of symmetric cells with impregnated Ag fired at 400 °C and loadings of 0.21 mg cm^{-2} (solid) and 0.46 mg cm^{-2} (hollow), respectively.

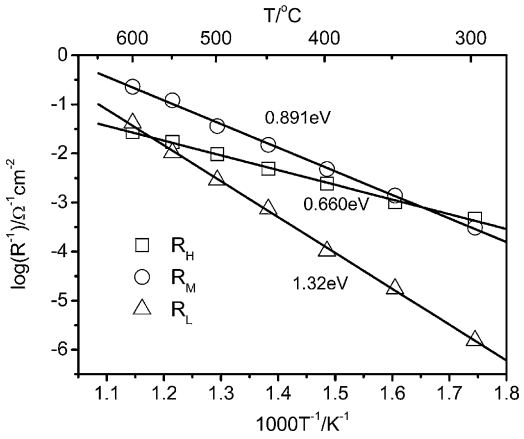

Fig. 7. Temperature dependence of fitted high frequency resistances, middle frequency resistances, and low frequency resistances of the symmetric cells with impregnated Ag fired at 600 °C and a loading of 0.46 mg cm^{-2}.

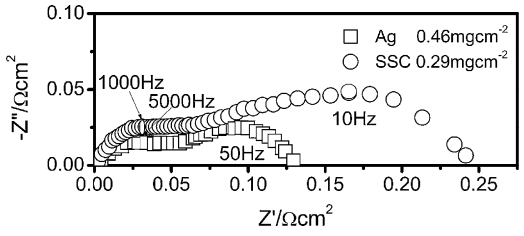

Fig. 8. Impedance spectra measured in air at 600 °C for symmetric cells with an impregnated Ag composite cathode (□) and an impregnated SSC composite cathode (○). The impregnated Ag and SSC were 0.46 mg cm^{-2} and 0.29 mg cm^{-2}, about 57 vol.%.

by single cells, as shown in Fig. 9. With humidified hydrogen as the fuel and stationary air as the oxidant, the open circuit voltages (OCV) are 1.13, 1.09 and 1.07 V, and the maximum power densities are 65, 127 and 283 mW cm^{-2} at 500, 550 and 600 °C, respectively. The maximum power density of the cell with an SSC-impregnated cathode is 239 mW cm^{-2} at 600 °C, about 16% lower than the value from an Ag-impregnated cathode. The high power density suggests that the Ag-impregnated cathode is a promising cathode for SOFC operating at low temperature and that higher power density can be achieved with Ag-impregnated cathodes with intensive reduction in electrolyte thickness.

The stability of impregnated cathodes was also studied, as shown in Fig. 10. Fig. 10(a) presents the long-term stability of a 0.46 mg cm^{-2} Ag (57 vol.%) impregnated cathode fired at temperatures between 400 and 600 °C and measured at 500 °C. The

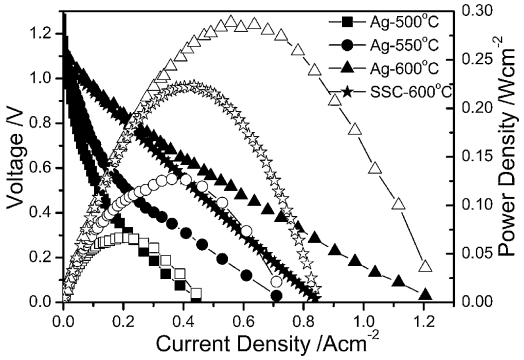

Fig. 9. *I–V* (solid) and *I–P* (hollow) curves for single cells with 0.46 mg cm^{-2} Ag-impregnated cathode and 0.29 mg cm^{-2} SSC-impregnated cathodes tested at various temperatures. The volume ratios of impregnated Ag and SSC are both about 57 vol.%.

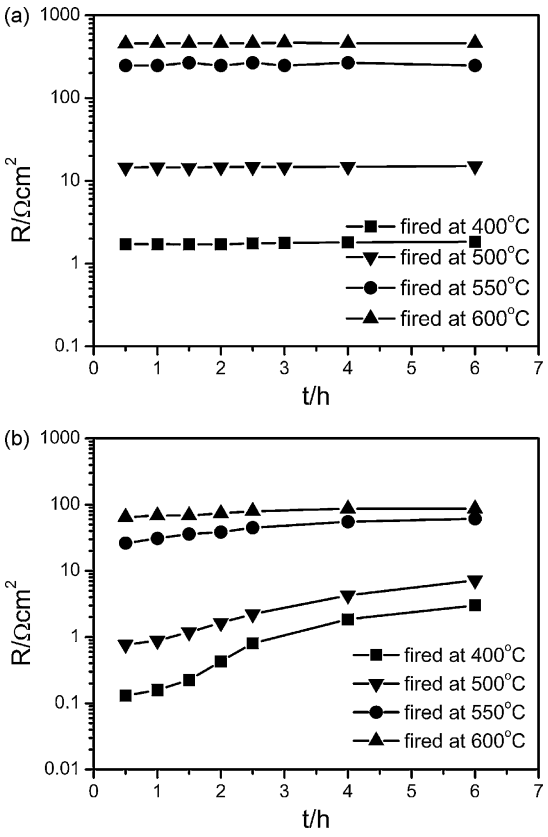

Fig. 10. The long-term stability of symmetric cells with 0.46 mg cm^{-2} Ag (57 vol.%) impregnated cathodes fired at different temperatures and tested in air at (a) 500 °C and (b) 600 °C.

polarization resistances increase with firing temperature, and no obvious decay was observed within the tested time. The polarization resistances measured at 600 °C increased largely with testing time, as shown in Fig. 10(b). The interfacial polarization resistances of the impregnated cathodes fired at 400 °C increase from 0.13 Ω cm^2 to 3.01 Ω cm^2 after a 6-h test, an increase of about 23-fold. The interfacial polarization resistances of cathodes fired at 600 °C also increased from 64.79 to 84.85 Ω cm^2, a change of about 30%.

Fig. 11 shows the microstructure of a 0.46 mg cm^{-2} Ag-impregnated cathode fired at 400 °C and tested at 600 °C for 12 h.

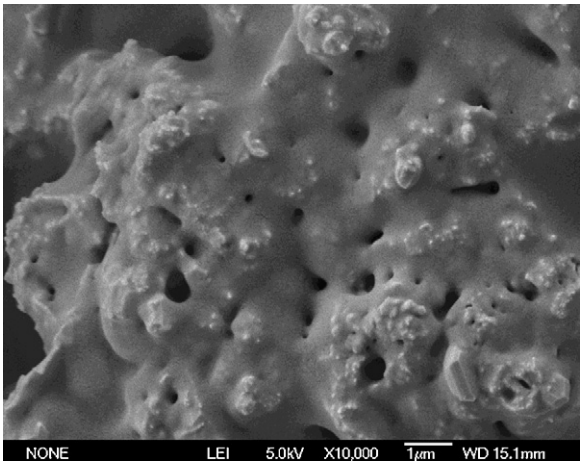

Fig. 11. SEM picture of a fractured cross-section of a 0.46 mg cm^{-2} Ag-impregnated cathode fired at 400 °C after testing at 600 °C for 12 h.

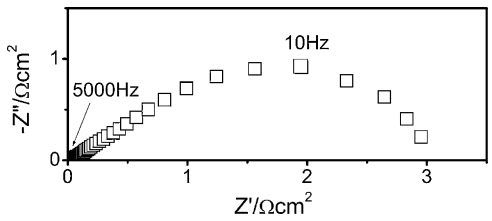

Fig. 12. Impedance spectrum of the 0.46 mg cm^{-2} Ag-impregnated cathode after testing at 600 °C for 12 h.

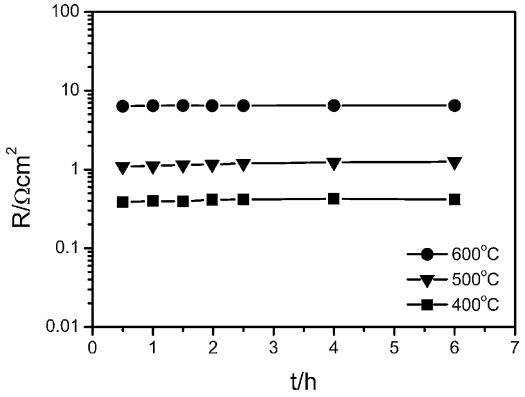

Fig. 13. Long-term stability of symmetric cells with Ag–Co_2O_3 co-impregnated cathodes fired at various temperatures and tested at 600 °C. The mole ratio of Ag^+ is 90%, and the Ag–Co_2O_3 loading is about 0.46 mg cm^{-2}.

After long-term testing, Ag particles aggregate due to their low melting point and form a dense amorphous cover on the BCS backbone, which results in low porosity and thus less TPBs. Fig. 12 shows the impedance spectra of the 0.46 mg cm^{-2} Ag-impregnated cathode fired at 400 °C and tested for 12 h at 600 °C. As shown in Fig. 12, R_H maintains about 0.06 Ω cm^2 after long-term testing, while R_L increases from 0.07 to 2.96 Ω cm^2. This result suggests that the transfer of dissociated O^- to TPBs becomes more severe due to the loss of porosity and TPBs length. The long-term test of Ag-impregnated cathode also suggests that the Ag-impregnated cathode is a promising cathode for fuel cells operating at temperatures lower than 600 °C.

Co-impregnation of Ag particles with some high-melting oxide particles, such as Co_2O_3, might be a good means of suppressing the aggregation of Ag particles at 600 °C. As shown in Fig. 13, between the firing temperature of 400 °C and the testing temperature of 600 °C, the Ag–Co_2O_3 loading was about 0.46 mg cm^{-2}, and the interfacial polarization resistances increase from 0.39 to 0.42 Ω cm^2 after a 6-h test, which is only 8% increased, making it much more stable than those with single Ag-impregnated cathodes. Better performance of co-impregnated cathodes would be achieved by optimizing their composition and microstructure as well as by adding other high-melting oxides, which calls for intensive future study.

4. Conclusions

An Ag–BCS composite cathode was fabricated by an ion impregnation technique. The Ag loading was hardly affected by Ag firing temperature, but the polarization resistances largely increased with Ag firing temperature. The minimum polarization resistance of symmetric cells was achieved with an Ag loading of 0.40 mg cm^{-2} and firing at 400 °C, with 0.11 Ω cm^2 at 600 °C. With the same volume ratio of 57%, the simulated high and low frequency resistances are 0.08 and 0.16 Ω cm^2 for SSC-impregnated cathodes as well as 0.06 and 0.07 Ω cm^2 for Ag-impregnated cathodes, suggesting that the reduction of low frequency resistances is the main reason for the decrease of polarization resistance in Ag-impregnated cathodes.

The 0.46 mg cm^{-2} Ag-impregnated cathode fired at 400 °C displayed maximum power densities of single cells up to 283 mW cm^{-2} at 600 °C. The long-term tests of Ag-impregnated cathodes also suggest that such cathodes are promising for fuel cells operating at temperatures below 600 °C.

Acknowledgement

This work was supported by the Natural Science Foundation of China (50602043, 50730002) and the National High Technology Research and Development Program of China (2007AA05Z157 and 2007AA05Z151).

References

[1] K.D. Kreuer, Annu. Rev. Mater. Res. 33 (2003) 333–359.
[2] D. Hirabayashi, A. Tomita, S. Teranishi, T. Hibino, M. Sano, Solid State Ionics 176 (2005) 881–887.
[3] R. Peng, Y. Wu, L. Yang, Z. Mao, Solid State Ionics 177 (2006) 389–393.
[4] R. Mukundan, P.K. Davies, W.L. Worrell, J. Electrochem. Soc. 148 (2001) A82–A86.
[5] Q. Ma, R. Peng, Y. Lin, J. Gao, G. Meng, J. Power Sources 161 (2006) 95–98.
[6] T. Wu, R. Peng, C. Xia, Solid State Ionics 179 (2008) 1505–1508.
[7] B. Lin, M. Hu, J. Ma, Y. Jiang, S. Tao, G. Meng, J. Power Sources 183 (2008) 479–484.
[8] L. Zhao, B. He, B. Lin, H. Ding, S. Wang, Y. Ling, R. Peng, G. Meng, X. Liu, J. Power Sources 194 (2009) 835–837.
[9] Z. Tao, L. Bi, L. Yan, W. Sun, Z. Zhu, Electrochem. Commun. 11 (2009) 688–690.
[10] F. He, T. Wu, R. Peng, C. Xia, J. Power Sources 194 (2009) 263–268.
[11] A. Nagy, G. Mestl, Appl. Catal. A: Gen. 188 (1999) 337–353.
[12] S. Kim, L.Y. Yang, A.J. Jacobson, B. Abeles, Solid State Ionics 106 (1998) 189–195.
[13] Y. Akimune, K. Matsuo, H. Higashiyama, K. Honda, M. Yamanaka, M. Uchiyama, M. Hatano, Solid State Ionics 178 (2007) 575–579.
[14] S.P. Jiang, W. Wang, Solid State Ionics 176 (2005) 1351–1357.
[15] S.P. Jiang, Mater. Sci. Eng. A 418 (2006) 199–210.
[16] T. Wu, Y. Zhao, R. Peng, C. Xia, Electrochim. Acta 54 (2009) 4888–4892.
[17] T. Hibino, A. Hashimoto, M. Suzuki, M. Sano, J. Electrochem. Soc. 149 (2002) A1503–A1508.
[18] J.X. Wang, L.P. Li, B.J. Campbell, Z. Lv, Y. Ji, Y.F. Xue, W.H. Su, Mater. Chem. Phys. 86 (2004) 150–155.